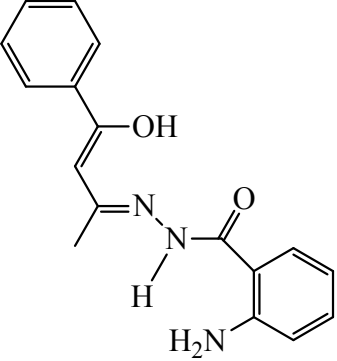
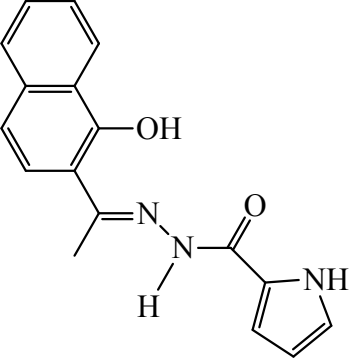
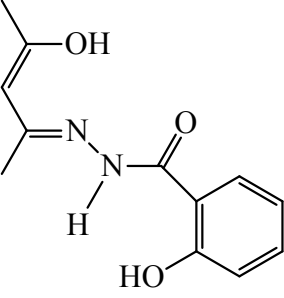
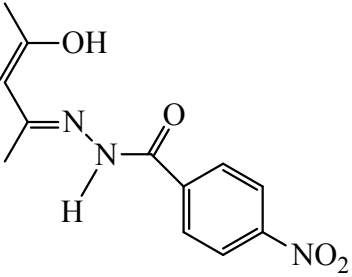
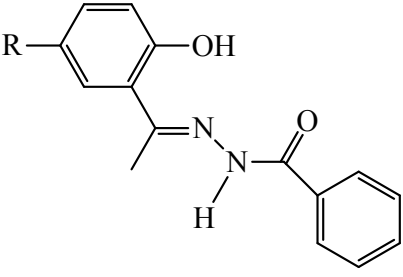
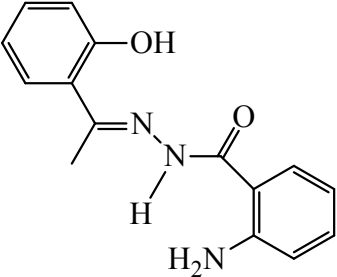
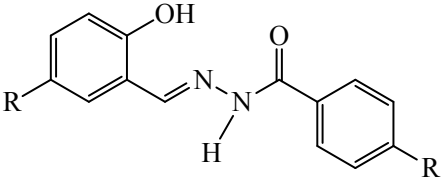
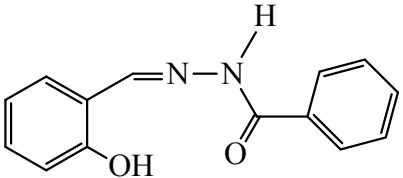
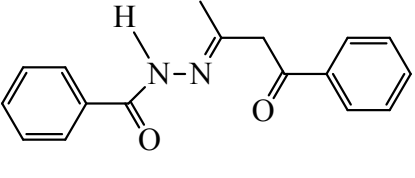
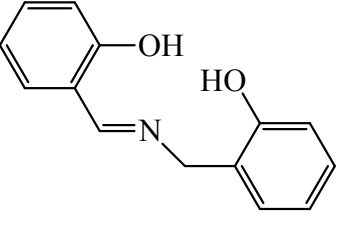
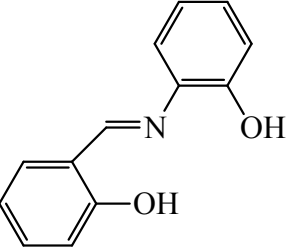
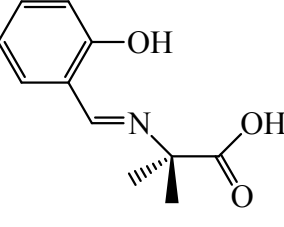


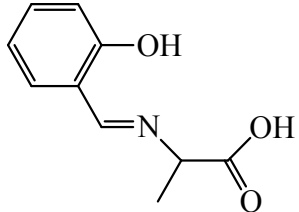
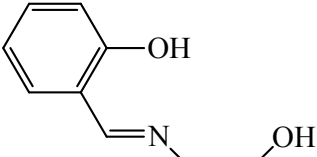
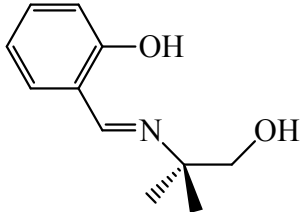
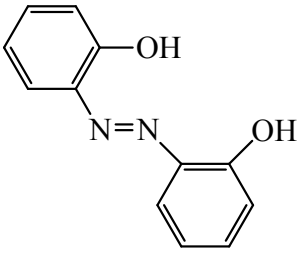
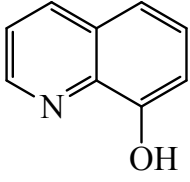
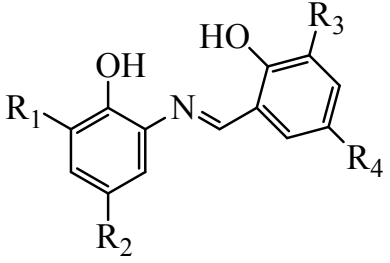
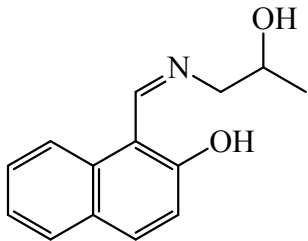
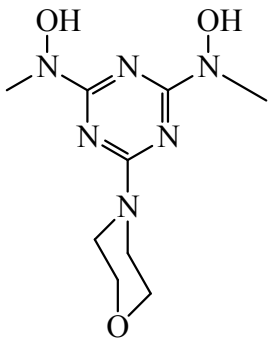
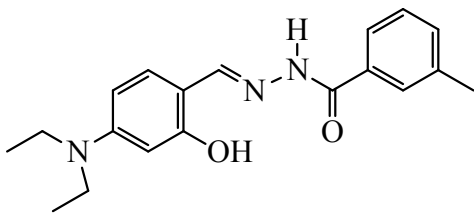
**DT-ART-09-2017-003585 (Revised)**

**Exploring the role of substituent in the hydrazone ligand of a family of  $\mu$ -oxidodivanadium(V) hydrazone complexes on structure, DNA binding and anticancer activity**

Debashis Patra,<sup>a</sup> Shubhabrata Paul,<sup>b</sup> Indira Majumder,<sup>b</sup> Nayim Sepay,<sup>c</sup> Sachinath Bera,<sup>d</sup> Rita Kundu,<sup>b</sup> Michael G. B. Drew,<sup>e</sup> and Tapas Ghosh\*,<sup>a</sup>

**Electronic Supporting Information (ESI)**

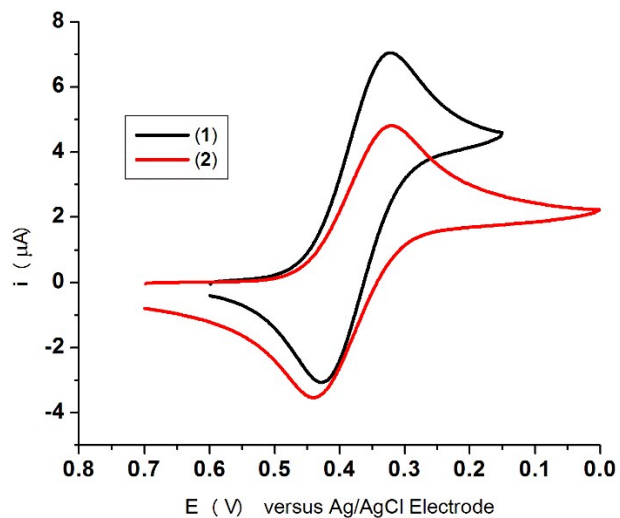
 <p>H<sub>2</sub>baah [Ref. 11(a)]</p>	 <p>H<sub>2</sub>naphpc [Ref. 11(b)]</p>	 <p>H<sub>3</sub>acsh [Ref. 11(c)]</p>
 <p>H<sub>2</sub>acnb [Ref. 11(d)]</p>	 <p>R = Me MeHapbh R = Cl ClHapbh</p> <p>[Ref. 11(e)]</p>	 <p>H<sub>2</sub>hapah [Ref. 11(f)]</p>
 <p>R = H, R' = H H<sub>2</sub>bhsH R = H, R' = OMe H<sub>2</sub>ahsH R = OMe, R' = H H<sub>2</sub>bhsOMe R = OMe, R' = OMe H<sub>2</sub>ahsOMe</p> <p>[Ref. 11(g)]</p>	 <p>H<sub>2</sub>salbh [Ref. 11(h)]</p>	 <p>H<sub>2</sub>babh [Ref. 11(i)]</p>
 <p>H<sub>2</sub>salamp [Ref. 12(a)]</p>	 <p>H<sub>2</sub>sal-amp [Ref. 12(b)]</p>	 <p>H<sub>2</sub>sal-L-val [Ref. 13(a)]</p>

 <p>H<sub>2</sub>sal-L-ala [Ref. 13(b)]</p>	 <p>H<sub>2</sub>salea [Ref. 14(a)]</p>	 <p>H<sub>2</sub>salamhp [Ref. 14(b)]</p>
 <p>H<sub>2</sub>dhab [Ref. 15]</p>	 <p>Hhq [Ref. 16]</p>	 <p>R<sub>1</sub>, R<sub>3</sub> = -H, R<sub>2</sub>, R<sub>4</sub> = -Cl, Cl-ono-Cl  R<sub>1</sub>, R<sub>3</sub> = -H, R<sub>2</sub> = tert-amyl, R<sub>4</sub> = tert-butyl tA-ono-tB  R<sub>1</sub> = -H, R<sub>2</sub> = tert-amyl, R<sub>3</sub>, R<sub>4</sub> = tert-butyl tA-ono-2tB</p> <p>H<sub>2</sub>XonoY [Ref. 17]</p>
 <p>H<sub>2</sub>imn [Ref. 18]</p>	 <p>H<sub>2</sub>bihyat [Ref. 19 &amp; 20]</p>	 <p>H<sub>2</sub>embh [Ref. 21]</p>

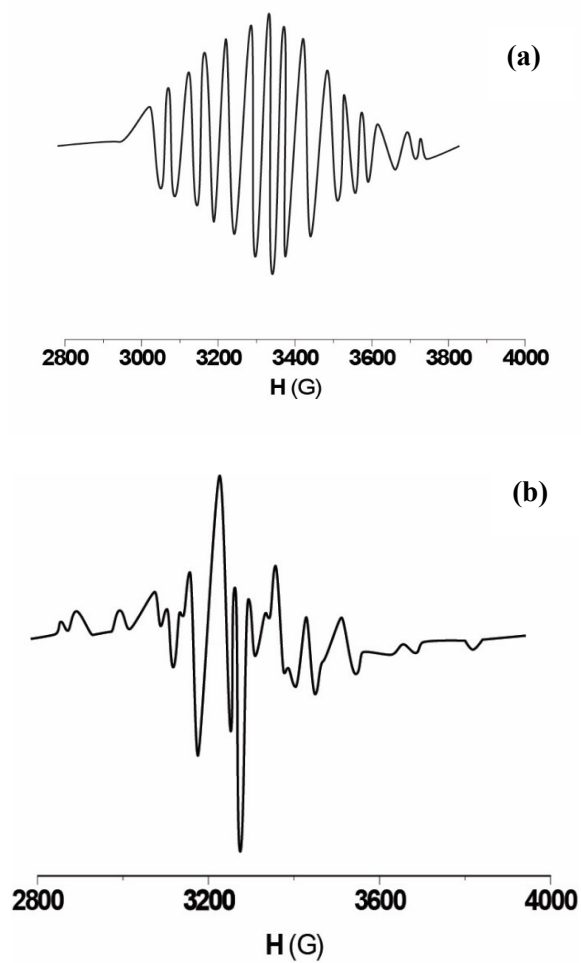
**Scheme S1.** The structure of the ligands present in the complexes mentioned in Table 4.

Table S1 Different type of interactions between the CT-DNA and HPV 18 DNA with the complexes obtained from molecular docking study.

Complex	VdW + H bond + dissolving energy	Electr ostatic energy	Total (1)	Final total internal energy (kcal mol <sup>-1</sup> ) (2)	Torsional free energy (kcal mol <sup>-1</sup> ) (3)	Unbound system's energy (4)	Estimated free energy of binding [(1) + (2) + (3) - (4)] (kcal mol <sup>-1</sup> )
CT DNA							
<b>1</b>	-8.53	-0.53	-9.06	-3.04	1.79	-3.04	-7.27
<b>2</b>	-10.87	-0.11	-10.98	-2.60	2.39	-2.60	-8.59
HPV 18 DNA							
<b>1</b>	-9.64	0.02	-9.62	-3.47	1.79	-3.47	-7.82
<b>2</b>	-10.74	-0.09	-10.83	-3.52	2.39	-3.52	-8.44



**Fig. S1.** Cyclic voltammogram of the complexes **1** and **2** in  $\text{CH}_2\text{Cl}_2$  solution.



**Fig. S2.** X-band EPR spectra of complex **1A** in  $\text{CH}_2\text{Cl}_2$  solution (a) at 300 K and (b) at 77 K.

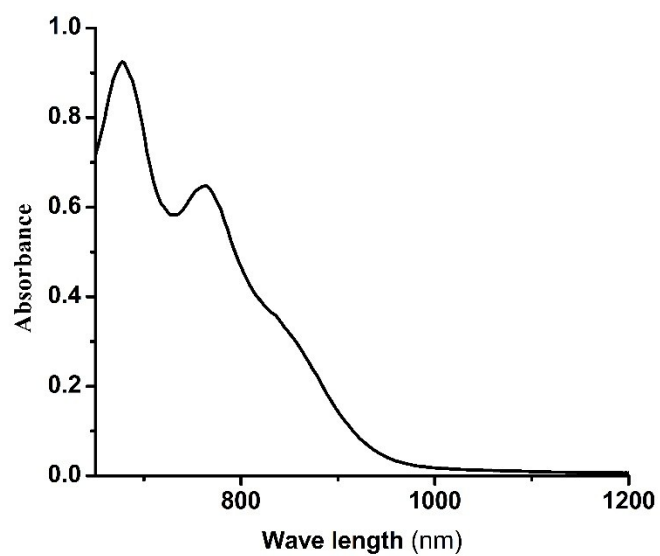


Fig. S3. Electronic spectra of 2A in CH<sub>2</sub>Cl<sub>2</sub> solution.

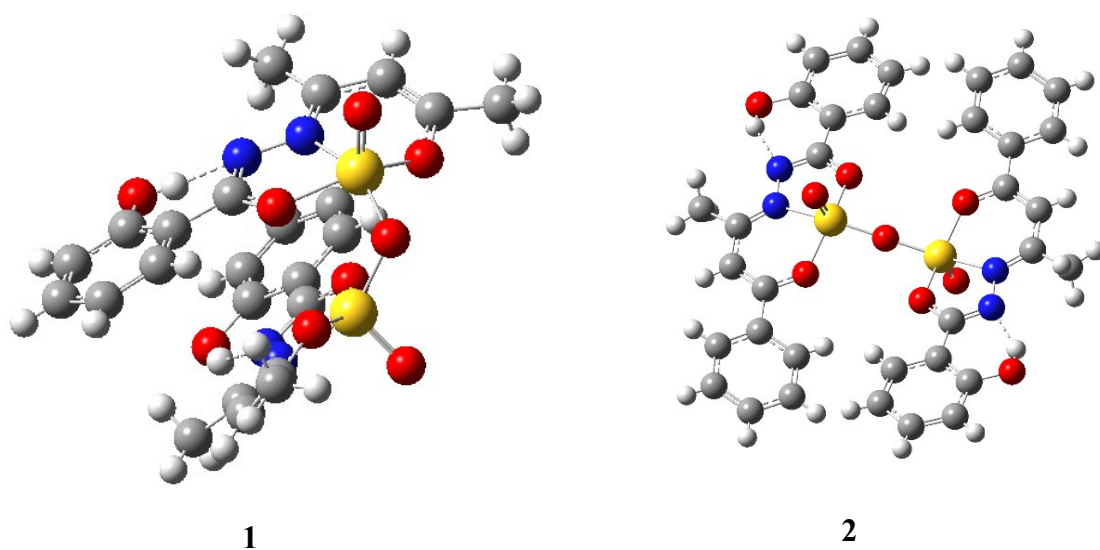
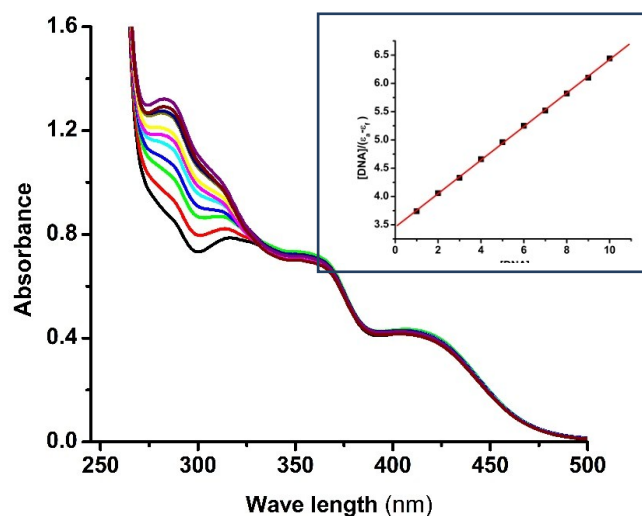
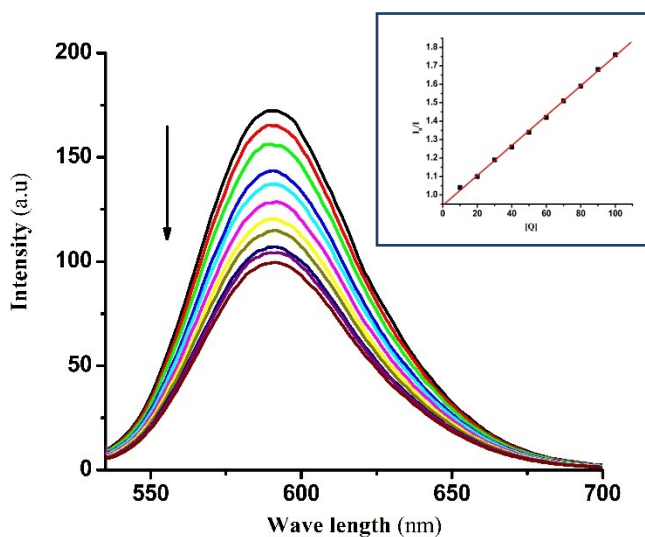


Fig. S4. DFT optimized structure of 1 and 2.



**Fig. S5.** Absorption spectra of the complex **2** in the presence of increasing amounts of CT DNA. A fixed concentration of complex ( $1.0 \times 10^{-5}$  M) was treated with increasing amounts of DNA over a range of  $(1-10) \times 10^{-6}$  M. (**inset:** The linear fit of  $[DNA]/(\epsilon_a - \epsilon_f)$  versus  $[DNA]$ ).



**Fig. S6.** Fluorescence spectra of (1st) EB +  $10^{-4}$  M DNA control and (2nd)-(11th) EB + DNA +  $(1-10) \times 10^{-5}$  M of complex **2**. The arrow shows that the intensity decreases with the increasing concentration of complex **2**. [**Inset:** Stern-Volmer plot for the quenching of fluorescence of the ethidium bromide (EB) DNA complex caused by complex **2**].

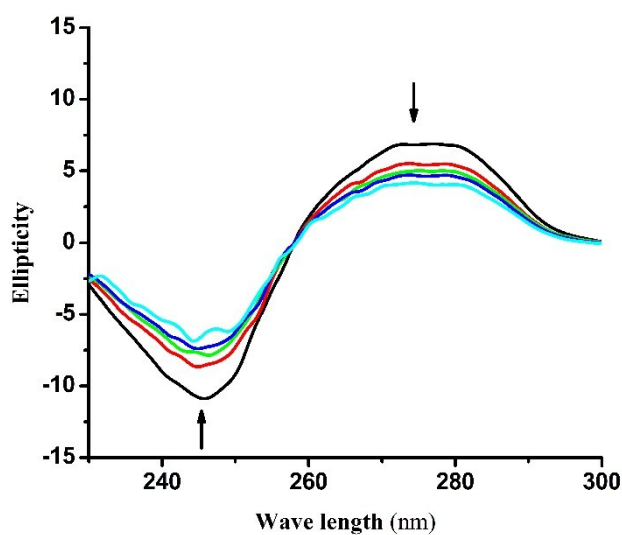


**Fig. S7** Circular dichroism spectra of 60  $\mu\text{M}$  CT-DNA in 10 mM Tris-HCl buffer (pH 7.2) titrated with of 10-40  $\mu\text{M}$  complex **2**. The scan rate of 50 nm/min was maintained and cuvette with 1 mm path length was used.

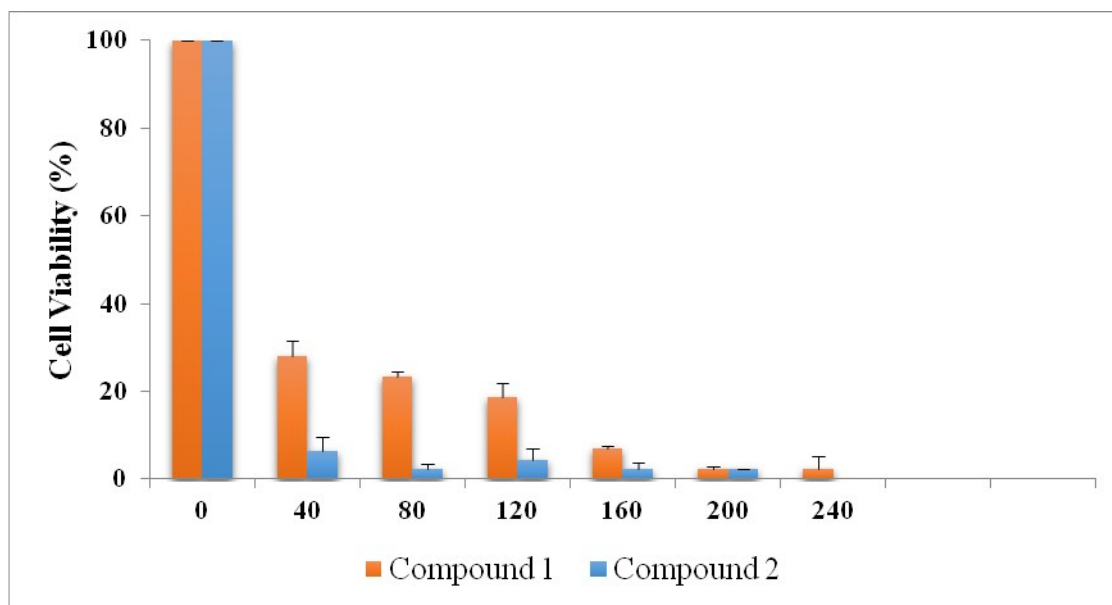
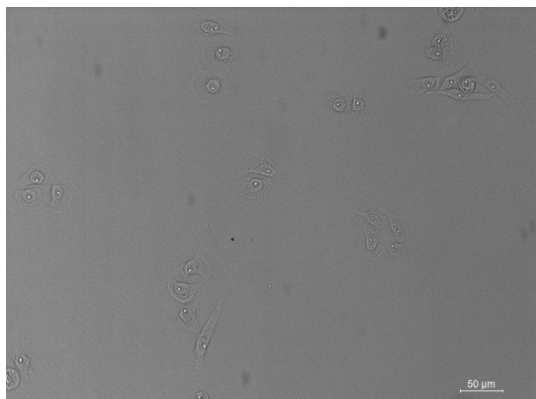


**Fig. S8** MTT assay showing cell viability of SiHa cells treated with complexes **1** and **2** (concentration range: 40-240  $\mu\text{M}$ ), bars represent SD of three independent replicates.

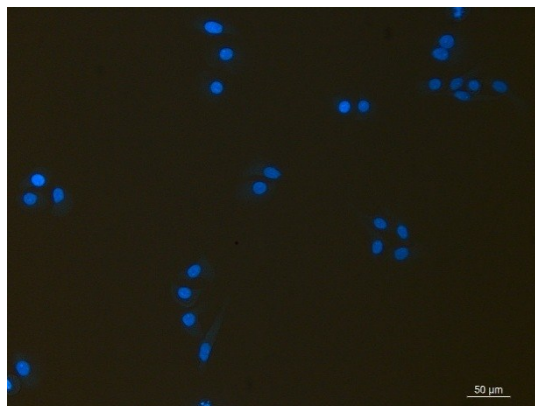


Bright field image



Control (a)

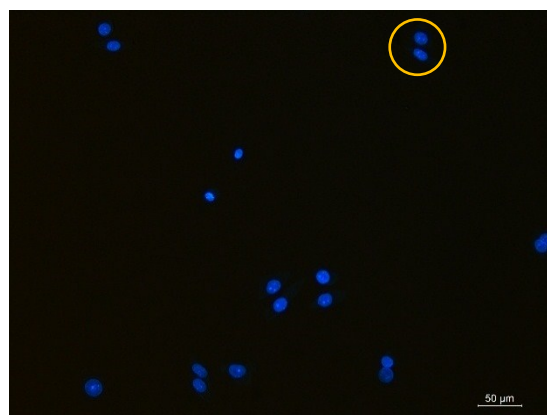
Blue florescence image



Control (b)



Complex 1 (a)



Complex 1 (b)

**Fig. S9.** Study of apoptosis by morphological changes in nuclei of SiHa cells. Marked circle showing the morphological changes in nuclei of SiHa cells observed on applying complex 1 in comparison to control.

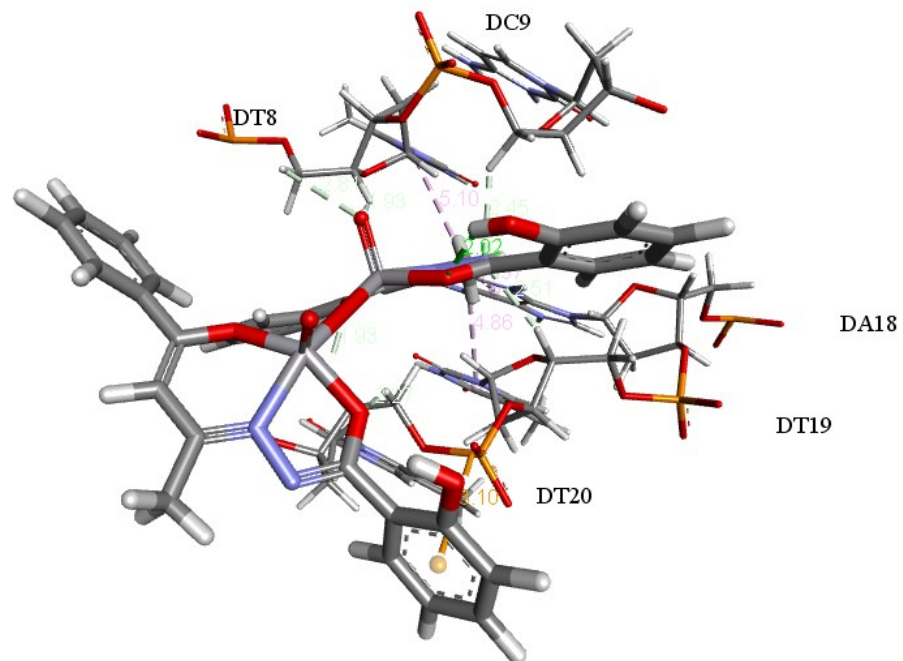


**Fig. S10.** Docked pose of complex **2** showing interaction with CT DNA base pairs.

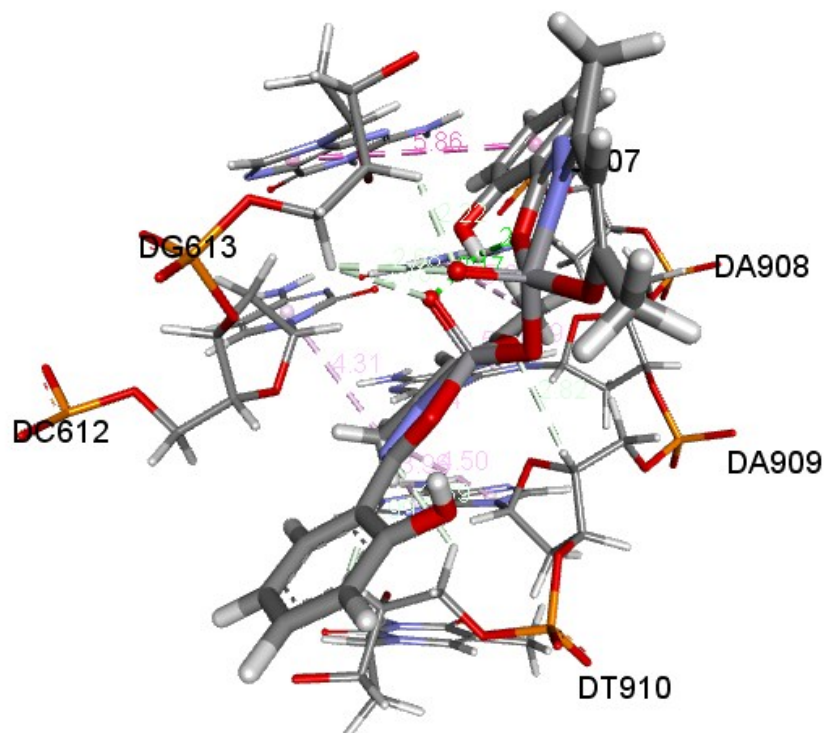


**Fig. S11.** Docked pose of complex **1** showing interaction with HPV 18 DNA base pairs.